Experimental research on the evaluation of left ventricular systolic function by layered speckle tracking before and after berberine treatment in a cardiac hypertrophy rat model

Haorou Luo[1#^], Tuli Kou[2#], Ye Su[3#], Yang Shen[4], Lixue Yin[5]

[1]Ultrasonic Imaging Department of Chengdu Women's and Children's Central Hospital, School of Medicine, University of Electronic Science and Technology of China, Chengdu, China; [2]Ultrasonic Imaging Department, Chengdu Second People's Hospital, Chengdu, China; [3]Department of Cardiovascular Ultrasound and Cardiac Function, Sichuan Provincial People's Hospital, School of Medicine, UESTC, Chengdu, China; [4]Department of Stomatology, Chengdu Seventh People's Hospital, Chengdu, China; [5]Sichuan Provincial Key Laboratory of Ultrasound Cardiac Electrophysiology and Biomechanics, Sichuan Academy of Medical Sciences, Sichuan Provincial People's Hospital, School of Medicine, UESTC, Chengdu, China

Contributions: (I) Conception and design: H Luo, T Kou; (II) Administrative support: L Yin, H Luo; (III) Provision of study materials or patients: L Yin, Y Su, Y Shen; (IV) Collection and assembly of data: H Luo, T Kou; (V) Data analysis and interpretation: H Luo, T Kou, Y Su; (VI) Manuscript writing: All authors; (VII) Final approval of manuscript: All authors.

[#]These authors contributed equally to this work and should be considered as co-first authors.

Correspondence to: Lixue Yin. Sichuan Provincial People's Hospital, School of Medicine, UESTC, Chengdu, China. Email: yinlixue_cardiac@163.com.

Background: To evaluate the effect of berberine (BBR) intervention on left ventricular hypertrophy and systolic function in rats by ultrasound layered strain imaging and cardiac hypertrophy model.

Methods: Eighty healthy male Sprague-Dawley (SD) rats were randomly divided into four groups: group A (normal saline control group), group B [isoproterenol (ISO) induced model group], group C (BBR hydrochloride 5 mg/kg + ISO group) and group D (BBR hydrochloride 10 mg/kg + ISO group). Echocardiography was performed on days 1, 7 and 14, respectively. The myocardial tissue was taken for pathological examination. The key proteins of Rho/ROCK signaling pathway were quantified by immunohistochemical staining.

Results: On day 7, compared with group A, peripheral strain values of the subendocardium and middle myocardium of rats in groups B, C and D were significantly decreased. The absolute value of circumferential strain (CS) in subendocardium and middle myocardium in group B was significantly lower than that in groups C and D (–24.21 *vs.* –26.68 *vs.* –27.69; –14.90 *vs.* –16.48 *vs.* –17.69). Pathological results showed that compared with the myocardial cells in control group A, the myocardial cells in group B had significantly increased cross-sectional area, and obvious myocardial interstitial fibrosis. Compared with group B, BBR intervention reduced the deposition of fibrosis in groups C and D, group D was more obvious. Immunohistochemical results showed that compared with group A, the protein expression levels of ROCK, RhoA and Bax in groups B, C and D were significantly increased, while the protein expression levels of Bcl-2 were significantly decreased.

Conclusions: Ultrasound layered strain imaging could evaluate the early left ventricular systolic function in isoprenaline-induced hypertrophy rat model. BBR might inhibit oxidative stress through the Rho/ROCK signaling pathway and slow down the progression of myocardial fibrosis after the formation of cardiac hypertrophy. This provides reference and direction for clinical decision-making and further research.

Keywords: Cardiac hypertrophy; layered strain; isoproterenol (ISO); berberine (BBR); echocardiography

---

^ ORCID: 0000-0002-1544-1349.

Introduction

Cardiac hypertrophy is a common clinicopathological outcome of cardiovascular diseases. Ventricular wall thickening and abnormal myocardial contractile ability are its early manifestations (1). The primary mechanism of the occurrence and development of heart failure is the cardiac remodeling theory. Cardiac hypertrophy is an essential part of cardiac remodeling and is an independent risk factor for increased prevalence and mortality of cardiovascular diseases (2). Early compensatory cardiac hypertrophy can maintain average blood circulation in the heart, but long-term cardiac hypertrophy can lead to cardiac dysfunction that increases the risk of sudden cardiac death (3). Therefore, it is highly important to improve the prognosis of patients by evaluating the morphological and functional changes of left ventricular hypertrophy in an early, effective, and accurate manner and providing patients with timely, accurate and effective treatment and efficacy evaluation.

Evaluation of myocardial deformation by speckle-tracking echocardiography has provided helpful information on local and global ventricular function (4), which can be used to evaluate the myocardial damage in experimental rats in various heart diseases (5). A typical left ventricular myocardium has three layers: endocardial myocardium, midwall myocardium and epicardial myocardium (6). The current speckle-tracking imaging (STI) technology studies mainly focus on the overall systolic function of the heart, while there are few studies on the role of the left ventricular three-layer myocardium (7,8).

The occurrence and development of cardiac hypertrophy are bound to involve the activation of cellular signaling pathways, among which the Rho/ROCK pathway has been mentioned repeatedly to be involved in the pathogenesis of ISO-induced cardiac hypertrophy (9). Presently, the specific mechanism of the occurrence and development of cardiac hypertrophy is still vague. Therefore, tracing the intracellular signaling pathway of cardiac hypertrophy may provide a new thinking direction for drug intervention. Berberine (BBR), derived from coptis chinensis, is an alkaloid with anti-cancer, anti-oxygen free radical, anti-bacterial, anti-hyperglycemia and other functions, and also has a particularly protective effect on myocardium (10). Che *et al.* (11) demonstrated that BBR preconditioning reduced isoproterenol (ISO)-induced TGF-β1 mRNA expression in macrophages and that BBR may play a protective role in cardiac injury by reducing macrophages. Tian *et al.* (12) found that BBR could effectively hinder the Rho/ROCK pathway and reduce oxygen free radicals in diabetic rats, thus protecting the brain barrier. Experiments were conducted experiments to verify our hypothesis that BBR can protect ISO-induced cardiac hypertrophy in rats by hindering the Rho/ROCK signaling pathway.

Focusing on that in the current study, we aimed to apply the STI-layered strain to detect cardiac dysfunction in a rat model of cardiac hypertrophy and reveal the abnormal features of cardiac mechanical function in the rat model of cardiac hypertrophy induced by ISO. The changes in left ventricular systolic function in rats were compared before and after drug intervention. Simultaneously, the protective effect of BBR on ISO-induced myocardial injury in rats was evaluated, and the molecular mechanism of its therapeutic effect was elucidated by studying related functional parameters and histological changes. We present the

---

Highlight box

Key findings

- Ultrasound layered strain imaging could evaluate the early left ventricular systolic function in isoprenaline-induced hypertrophy rat model. Berberine could slow down the progression and deterioration of myocardial fibrosis after the formation of cardiac hypertrophy. The mechanism of action might be due to the inhibition of the Rho/ROCK signaling pathway.

What is known and what is new?

- This was the first study to use layered strain to assess systolic function before and after berberine intervention in a rat model of cardiac hypertrophy. We successfully detected the cardiac dysfunction in the rat model of early cardiac hypertrophy by layered strain imaging.

What is the implication, and what should change now?

- This study may provide an ultrasound imaging technology platform for further application of rat models to study related cardiovascular diseases. The number of experimental cases is small, and the correlation between layered strains and clinical application of berberine needs to be further confirmed by large-scale clinical trials in the future.

---

following article in accordance with the ARRIVE reporting checklist (available at https://cdt.amegroups.com/article/view/10.21037/cdt-22-464/rc).

Methods

Animals

Experiments were performed under a project license (No. 27-2021) granted by the Ethics Committee of University of Electronic Science and Technology of China, in compliance with our institutional guidelines for the care and use of animals. Male Sprague-Dawley (SD) rats [Grade II, Certificate No. SCXK (Chuan) 2020-030] were purchased from Chengdu Dasuo Experimental Animal Co., Ltd. (Chengdu, China). About 10 weeks old, 250 g mature rats were kept at the Medical Animal Center of the Sichuan Provincial People's Hospital. Rats were reared in a specific pathogen-free environment. The temperature of the feeding room was maintained at about 25 ℃ and the relative humidity was 60%. The 12-hour light/dark environment was automatically set. Rats were routinely fed and drank unlimited amounts of water.

Establishment of cardiac hypertrophy model

Eighty rats were randomly divided into 4 groups with 20 rats in each group: group A (normal saline control group), group B (2 mg/kg ISO model group), group C (2 mg/kg ISO + 5 mg/kg BBR) and group D (2 mg/kg ISO + 10 mg/kg BBR). After 1 week of adaptive feeding, rats in groups B, C and D were intervened according to the modeling and treatment settings of each group, and were injected once a day for 14 consecutive days. Meanwhile, rats in group A were intraperitoneally injected with the same volume of normal saline. During the administration period, the changes of body weight of rats were recorded daily, and attention was paid to observe whether the rats showed signs of listlessness, reduced eating, abnormal bowel and urine.

Echocardiography

Echocardiography was performed at the end of each trial session (before modeling, and the seventh day of intervention, and the fourteenth day of intervention); 10% chloral hydrate was injected intraperitoneally for anesthesia. The left side was supine, the skin was shaved, and the electrocardiogram was connected. Then, an operator blinded to animal experimental group used GE, Vivid, E9 color Doppler ultrasound diagnostic instrument (General Electric Company Vivid, E9, Boston, USA) with an M12S transducer and frequency of 10–12 MHz, selecting the rodent program. Frame rate was 133 Hz, gain was 20–25 dB, depth was approximately 20 mm. Previously stored images were processed by image analysis software (EchoPAC V201; GE Healthcare, Boston, USA) for an offline evaluation. Left ventricular end-diastolic diameter (LVEDD), left ventricular end-systolic diameter (LVESD), end-diastolic septum thickness [interventricular septum (IVS)], left ventricular posterior wall thickness (LVPWD), left ventricular ejection fraction (LVEF) were calculated for each rat. Heart rate (HR) was determined from an M-shaped image taken at the level of the medial nipple in the short axis view of the left ventricle. Relative left ventricular wall thickness (RWT) = (2 × LVPWD)/LVEDD. All parameters were measured three times, and the average value was taken for analysis.

Layered speckle tracking echocardiography

We obtained 10 short-axis views of the left ventricular papillary muscles of stable cardiac cycles and imported them into the EchoPAC workstation. After selecting the clearest endocardium image, manually outline the endocardium contour, click to track automatically, and then adjust the region of interest to match the endocardium and epicardial myocardium. Finally, the endocardial layer circumferential strain (CS), the middle layer CS, and the epicardial myocardial layer CS were recorded. All data were measured three times, and the average value was taken for statistical analysis.

Histopathological analysis

After echocardiography, the rats were anesthetized and the hearts were removed. Five rats in each group were properly euthanized (intraperitoneal injection of ketamine at 120 mg/kg, followed by cervical dislocation). The apex of the heart was cut off and repeatedly rinsed with 0.9% normal saline. Myocardial tissue at the level of papillary muscle was fixed in 4% paraformaldehyde (PFA)/phosphate buffer solution (PBS) solution and stored in a refrigerator at 4 ℃ for 24 h. It was then dehydrated, embedded, and paraffin sectioned. After the patch was dewaxed and rehydrated, Masson trichromatic staining and hematoxylin-eosin staining were performed. Myocardial interstitial fibrosis (excluding

vascular space) was assessed on Masson trichrome staining. Two independent investigators performed threshold processing on the red-green-blue superposition Image of Masson tricolor section using Image-Pro Plus 6.0 Image analysis system to determine the total tissue area of myocardial fibrosis. Through hematoxylin-eosin staining, the pathological changes of myocardial tissue cells were observed under light microscope by experienced pathologists, and the results were judged and analyzed.

Immunohistochemical staining

ROCK1 (primary polyclonal rabbit antibody, the Affinity Biosciences Cat# AF7016, RRID: AB_2835321) Rho-A (primary polyclonal rabbit antibody, the Affinity Biosciences Cat# AF6352, RRID: AB_2835157) Bax (primary polyclonal rabbit antibody, the Affinity Biosciences Cat# bs-0127R, RRID: AB_2833304) BCL-2 (primary polyclonal rabbit antibody, the Affinity Biosciences Cat# bs-20351, RRID: AB_2835021) was used for IHC staining of the next series of sections. The required myocardial tissue images were acquired with a Pannoramic 250 digital slice scanner, and two independent investigators recorded and analyzed the integrated optical density (IOD) and area of the acquired images through the Image-pro Plus 6.0 image analysis system. According to the calculation of the average optical density, the average IOD of each sample was obtained by averaging the IODs of the 3 images obtained according to the law, and the percentage of fibrous tissue expression area was determined.

Statistical analysis

The continuous variable of a normal distribution was expressed as mean ± standard deviation. Non-normally distributed variables were expressed as the median. Kolmogorov-Smirnov test was used to verify that the continuous variable was normally distributed. Homogeneity of variance was evaluated by Levene's test. The two groups of data were tested by a t-test of independent samples. Paired t-test was used to compare the data before and after. If the data for continuous variables satisfied normal distribution and homogeneity of variance, one-way analysis of variance (ANOVA) model was used, and the comparison among groups were performed with LSD method; Otherwise, the Kruskal-Wallis test was performed to compare the differences of the non-conforming measurement data. The correlation between CS of subendocardial myocardium (Endo-CS) and other strain values and the percentage of myocardial collagen fiber deposition was analyzed by Pearson or Spearman correlation coefficient, and Spearman correlation coefficient was calculated. All statistical analyses were performed on SPSS 25.0 for Mac and all statistical tests were double-sided. P value <0.05 was considered statistically significant.

During the allocation, the conduct of the experiment, the outcome assessment, and the data analysis, were done without the knowledge of each other.

Results

Rat model

Four rats in the ISO group died during the modeling process, so the final number of rats in the ISO group was as follows: group A 20, group B 16, group C 17, and group D 19. Cardiac hypertrophy was successfully induced in 52 rats and confirmed by histological analysis.

Parameters of conventional two-dimensional echocardiography

There were no statistically significant differences in body weight and HR of experimental rats in groups A, B, C and D at three time points before administration, on day 7 of intervention and on day 14 of intervention (P>0.05, as shown in *Table 1*).

Before administration: there were no statistically significant differences in IVS, LVPW, RWT and ejection fraction (EF) among the four groups (P>0.05, as shown in *Table 1*). On day 7 of administration: compared with group A, IVS and LVPW in groups B, C and D were significantly increased, with statistical significance (2.15 *vs.* 3.33 *vs.* 2.90 *vs.* 2.51; 2.08 *vs.* 2.26 *vs.* 2.20 *vs.* 2.15; P<0.001). The IVS and LVPW of C and D groups were significantly lower than those of group B, and the differences were statistically significant (P<0.001), the IVS of group C was higher than that of group D (2.90 *vs.* 2.51; P=0.017). On day 14 of administration: compared with group A, EF, IVS, LVPW and RWT in groups B, C and D were significantly decreased, and IVS, LVPW and RWT were significantly increased, with statistical significance (P<0.05). Compared with group B, group C and D had higher EF, lower IVS, LVPW and RWT (P<0.05). Compared with group C, group D had higher EF and lower IVS, and the differences were statistically significant.

Table 1 Basic characteristics and conventional ultrasound indicators

Groups	Weight (g)	Heart rate (beats/min)	IVS (mm)	LVPW (mm)	RWT	EF%
Group A						
Day 0 (n=20)	251.37±4.36	259±5	2.14±0.06	2.08±0.07	0.79±0.09	94.30±2.45
Day 7 (n=20)	291.40±3.75	259±6	2.15±0.07[abc]	2.08±0.07[abc]	0.79±0.10	94.65±2.32
Day 14 (n=20)	333.86±5.24	259±6	2.15±0.07[abc]	2.08±0.07[abc]	0.79±0.10[abc]	94.60±2.30[abc]
Group B						
Day 0 (n=20)	252.55±4.14	259±7	2.14±0.05	2.09±0.06	0.78±0.06	94.44±2.39
Day 7 (n=16)	291.11±3.68	259±6	3.33±0.15[ade]	2.26±0.09[ade]	0.85±0.07	94.44±1.63
Day 14 (n=16)	331.81±4.62	259±6	4.59±0.29[ade]	2.66±0.16[ade]	1.00±0.10[ade]	81.50±3.22[ade]
Group C						
Day 0 (n=20)	252.18±3.78	261±7	2.14±0.06	2.09±0.06	0.79±0.06	94.47±1.62
Day 7 (n=17)	292.17±3.33	261±7	2.90±0.11[bdf]	2.20±0.05[bd]	0.83±0.05	94.41±2.29
Day 14 (n=17)	332.74±8.52	260±6	3.35±0.16[bdf]	2.30±0.07[bd]	0.88±0.06[bd]	85.41±2.50[bdf]
Group D						
Day 0 (n=20)	253.10±3.96	259±6	2.15±0.08	2.08±0.07	0.78±0.07	94.32±2.16
Day 7 (n=19)	292.39±3.15	261±5	2.51±0.15[cef]	2.15±0.06[ce]	0.81±0.06	93.53±1.93
Day 14 (n=19)	333.03±9.76	260±6	2.95±0.08[cef]	2.25±0.05[ce]	0.85±0.06[ce]	89.42±1.74[cef]

Data are shown as mean ± standard deviation. [a], group A *vs.* group B P<0.05; [b], group A *vs.* group C P<0.05; [c], group A *vs.* group D P<0.05; [d], group B *vs.* group C P<0.05; [e], group B *vs.* group D P<0.05; [f], group C *vs.* group D P<0.05. IVS, interventricular septum; LVPW, left ventricular posterior wall; RWT, relative wall thickness; EF, ejection fraction.

Intra-group comparison: IVS, LVPW, EF and RWT values in control group did not change significantly with prolonged administration time (P>0.05). IVS, LVPW and RWT values of rats in ISO group increased continuously with prolonged administration, and there was significant statistical difference between baseline and 14th day after administration, while EF value decreased significantly on 14th day after administration, which was also confirmed by histopathological examination. IVS, LVPW and RWT values of rats in group C and group D increased from baseline on day 7 to 14 (P<0.05), while EF value did not change significantly from baseline on day 7 and decreased significantly from baseline on day 14 (P<0.05).

Layered speckle tracking echocardiographic parameters

Before administration: there was no statistical difference in the circumferential layered strain values at the level of the left ventricular short-axis papillary muscle between the groups B, C, D and the normal control group. On day 7 of administration: compared with group A, the overall Endo-

CS, the overall CS of middle myocardium (Mid-CS) and left. The overall CS values at the ventricular short-axis papillary muscle level were significantly decreased (P<0.001). Compared with group A, the overall CS value of epicardial myocardium (Epi-CS) of the subepicardial myocardium of rats in groups B, C, and D decreased, but the difference was not statistically significant (P>0.05). Endo-CS and Mid-CS in groups C and D were significantly higher than those in group B (–24.21 *vs.* –26.68 *vs.* –27.69; –14.90 *vs.* –16.48 *vs.* –17.69; P<0.001). Compared with the Endo-CS and Mid-CS of group C and group D, group C was lower than group D, but there was no statistical difference (P>0.05, as shown in *Table 2*). On day 14 of administration: compared with group A, Endo-CS, Mid-CS, Epi-CS, and global circumferential strain (GCS) of rats in group B, C, and D were significantly decreased (P<0.001). These strain values in groups C and D were significantly higher than those in group B (P<0.001). Compared with the Endo-CS and Mid-CS of group C and group D, group C was lower than group D, and there was a statistical difference at this time (P=0.001; P=0.025, as shown in *Table 3*).

Table 2 Comparison of circumferential layered strain on the 7th day

Groups	Indicators	Baseline	Day 7	P value
A	Endo-CS	−29.51±1.50	−29.57±1.53[abc]	0.218
	Mid-CS	−19.36±2.84	−19.39±2.82[abc]	0.33
	Epi-CS	−12.42±2.57	−12.40±2.60	0.33
	GCS	−20.43±1.75	−20.46±1.75[abc]	0.171
B	Endo-CS	−29.31±1.75	−24.21±2.07[ae]	<0.001
	Mid-CS	−19.37±2.29	−14.90±1.65[ae]	<0.001
	Epi-CS	−12.44±2.83	−11.64±2.22	0.154
	GCS	−20.38±1.82	−16.92±1.51[ade]	<0.001
C	Endo-CS	−29.41±1.34	−26.68±1.54[bf]	<0.001
	Mid-CS	−19.35±1.91	−16.48±1.81[bf]	<0.001
	Epi-CS	−12.41±2.35	−11.68±2.13	0.382
	GCS	−20.39±1.33	−18.29±1.42[bd]	<0.001
D	Endo-CS	−29.46±1.19	−27.69±1.06[cef]	<0.001
	Mid-CS	−19.36±1.41	−17.69±1.67[ef]	<0.001
	Epi-CS	−12.38±1.90	−11.69±1.76	<0.217
	GCS	−20.42±1.18	−19.03±1.08[ce]	<0.001

Data are shown as mean ± standard deviation. [a], group A *vs.* group B P<0.05; [b], group A *vs.* group C P<0.05; [c], group A *vs.* group D P<0.05; [d], group B *vs.* group C P<0.05; [e], group B *vs.* group D P<0.05; [f], group C *vs.* group D P<0.05. CS, circumferential strain; GCS, global circumferential strain.

Table 3 Comparison of circumferential layered strain on the 14th day

Groups	Indicators	Baseline	Day 7	P value
A	Endo-CS	−29.51±1.50	−29.50±1.34[abc]	0.929
	Mid-CS	−19.36±2.84	−19.24±2.84[ab]	0.590
	Epi-CS	−12.42±2.57	−12.37±2.60[abc]	0.727
	GCS	−20.43±1.75	−20.37±1.71[abc]	0.644
B	Endo-CS	−29.31±1.75	−21.06±1.39[ade]	<0.001
	Mid-CS	−19.37±2.29	−12.22±1.31[ade]	<0.001
	Epi-CS	−12.44±2.83	−8.66±1.82[ae]	<0.001
	GCS	−20.38±1.82	−13.98±0.90[ade]	<0.001
C	Endo-CS	−29.41±1.34	−24.29±1.44[bdf]	<0.001
	Mid-CS	−19.35±1.91	−14.72±1.83[bdf]	<0.001
	Epi-CS	−12.41±2.35	−10.08±1.77[b]	0.001
	GCS	−20.39±1.33	−16.36±1.34[bd]	<0.001
D	Endo-CS	−29.46±1.19	−25.74±0.62[cef]	<0.001
	Mid-CS	−19.36±1.41	−16.56±1.67[ef]	<0.001
	Epi-CS	−12.38±1.90	−10.46±1.21[ce]	<0.001
	GCS	−20.42±1.18	−17.58±0.90[ce]	<0.001

Data are shown as mean ± standard deviation. [a], group A *vs.* group B P<0.05; [b], group A *vs.* group C P<0.05; [c], group A *vs.* group D P<0.05; [d], group B *vs.* group C P<0.05; [e], group B *vs.* group D P<0.05; [f], group C *vs.* group D P<0.05. CS, circumferential strain; GCS, global circumferential strain.

Intra-group comparison: Endo-CS and Mid-CS values of ISO group continued to decrease with the prolongation of administration time. Compared with the baseline on the 14th day after administration, there was a statistically significant difference in the degree of reduction, while Epi-CS value on the 7th day did not change significantly compared with the baseline, but on the 14th day it was significantly lower than the baseline (P<0.05). On the 7th day, the Epi-CS value did not change significantly compared with the baseline, and on the 14th day, it decreased significantly (P<0.05).

The layered strain at the level of the left ventricular short-axis papillary muscle in groups A, B, C, and D showed gradient characteristics: the Endo > the Mid > the Epi (*Figure 1*).

Histological analysis

Compared with the cardiomyocytes of the rats in the control group A, the cardiomyocytes of the rats in the groups B, C, and D had different degrees of increased cross-sectional area, disordered arrangement, widened intercellular spaces, and increased interstitial fibrosis (as shown in *Figure 2*). The myocardial tissue pathological sections of rats in group B confirmed that the ISO-induced cardiac hypertrophy was successfully modeled.

Compared with rats in group A (1.05%±0.05%), rats in group B (27.74%±2.98%) had significantly increased fibrosis after 14 days (P<0.001, as shown in *Figure 3*). Compared with group B, BBR intervention reduced fibrotic deposition in groups C and D (24.87%±0.33% *vs.* 27.74%±2.98%; 20.29%±0.59% *vs.* 27.74%±2.98%, P<0.01), and decreased in group D more obvious.

Spearman rank correlation analysis was used to analyze the relationship between the layered strain value and the percentage of myocardial interstitial fiber deposition (Q%). The results showed that Endo-CS was positively correlated with the percentage of myocardial interstitial fiber deposition (r=0.805, P<0.001, as shown in *Figure 4*), and Mid-CS was positively correlated with the percentage of myocardial interstitial fiber deposition (r=0.758, P<0.001), as shown in *Figure 4*. Epi-CS was positively correlated with the percentage of myocardial interstitial fiber deposition, and the correlation was low and not statistically significant (r=0.345, P=0.136).

Reproducibility of STI

Sixteen studies were randomly selected to evaluate interobserver reproducibility of Endo-CS after gavage. To test variability between observers, the second observer analyzed the data without knowing the first observer's measurements. The results for reproducibility showed that the correlation coefficient was 0.885 (P<0.001), greater than 0.75, and the reproducibility of the test was good.

Comparison of heart mass

According to the rat heart mass and body weight, the mass index [heart weight/body weight (HW/BW)] was calculated. Compared with the HW/BW of rats in group A, the HW/BW of rats in groups B, C, and D were significantly higher (2.51 *vs.* 3.70 *vs.* 3.18 *vs.* 2.76, P<0.001). HW/BW in group B was higher than that in groups C and D (3.70 *vs.* 3.18, 3.70 *vs.* 2.76, P<0.001). HW/BW in group D was lower than that in group C (P<0.001).

Rho/ROCK signaling pathway related proteins

The expression of Rho/ROCK signaling pathway-related proteins was detected by immunohistochemistry, and the average optical density value was calculated to reflect the protein expression content semi-quantitatively. The experimental results showed that compared with group A, the expressions of ROCK, RhoA, and Bax proteins in groups B, C, and D were enhanced, while the expression of Bcl-2 protein was significantly decreased; The expression of RhoA, ROCK and Bax was not as high as that in group B; the expression of RhoA, ROCK and Bax in group D was lower than that in group C. The specific results are shown in *Table 4* and *Figures 5-8*.

Discussion

In this animal model of induced cardiac hypertrophy, it was demonstrated that continuous cardiac hypertrophy leads to significant myocardial fibrosis and necrosis. BBR could slow down the progression and deterioration of myocardial fibrosis after the formation of cardiac hypertrophy. The mechanism of action might be due to the inhibition of the Rho/ROCK signaling pathway and the changes in the expressions of downstream target factors Bax and Bcl-2, thereby inhibiting oxidative stress, and finally achieving the effect of improving cardiac hypertrophy. We also demonstrated that speckle tracking-based layered strain imaging parameters, especially subendocardial myocardial strain, were strongly associated with changes in myocardial
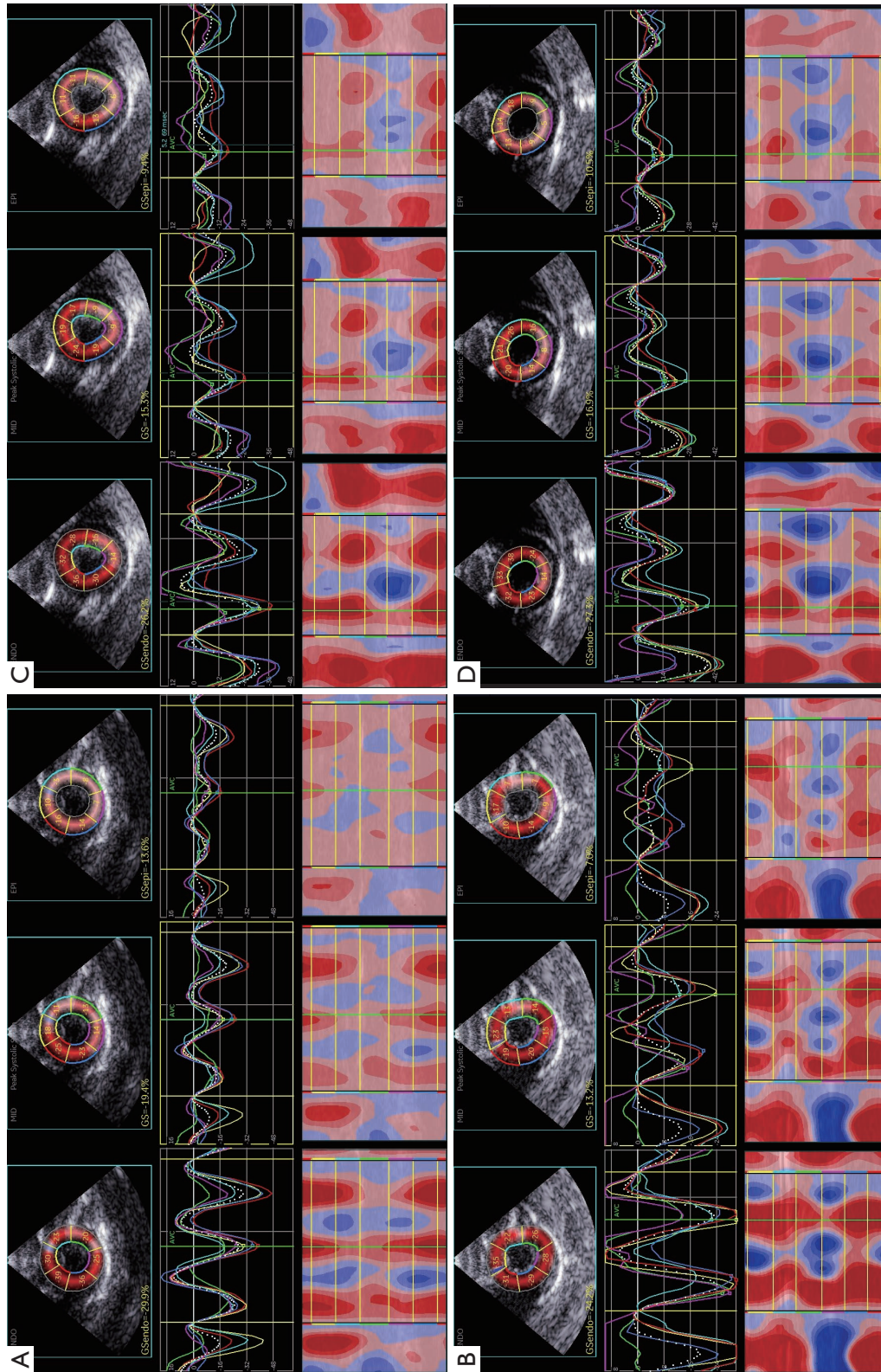
Figure 1 Layered strain at the level of the left ventricular short-axis papillary muscle in four groups of rats (day 7). (A) Group A rats; (B) group B rats; (C) group C rats; (D) group D rats. GS, global strain; Endo, endocardial myocardium; Mid, midwall myocardium; Epi, epicardial myocardium; AVC, aortic valve cloure (strain value at aortic closure).
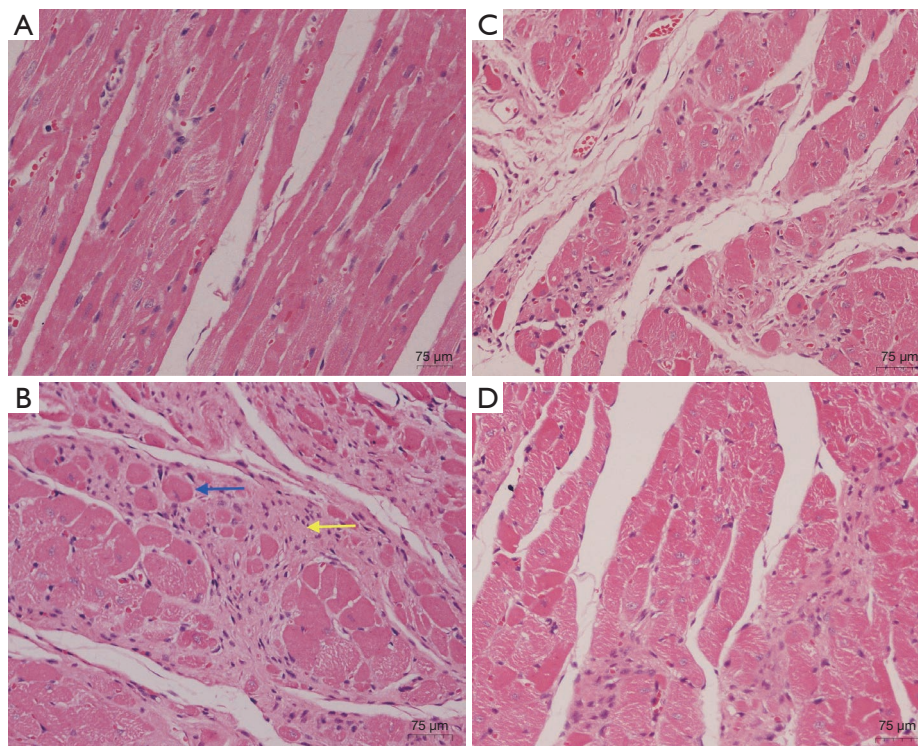
Figure 2 The results of HE staining of the rat myocardium in the four groups. (A) Rats in group A (the cardiomyocytes are uniform in size and neatly arranged); (B) rats in group B (blue arrow: hypertrophic cardiomyocytes; yellow arrow: myocardial fibrosis); (C) rats in group C (cardiomyocytes partial hypertrophy, slightly narrowed intercellular space, and smaller fibrosis area than group B); (D) rats in group D (with the same size of cardiomyocytes, slightly narrowed intercellular space, and smaller fibrosis area than group C). HE, hematoxylin and eosin.

interstitial fibrosis compared with traditional parameters of left ventricular ejection fraction.

To the best of our knowledge, there is no report in the literature on the evaluation of left ventricular systolic function in an animal model of cardiac hypertrophy by layered strain imaging technology. Based on the previous series of experiments, the animal model of cardiac hypertrophy in this study was made by intraperitoneal injection of ISO without opening the chest. Myocardial pathological staining of the rats taken out after 14 days confirmed that the cardiac hypertrophy and myocardial fibrosis were evident in the ISO group. Weighed with an electronic balance and calculated HW/BW. It was found that compared with the control group, the ISO group had a significantly higher HW/BW (3.70 *vs.* 2.51; P<0.001). Conventional transthoracic echocardiography exhibited increased interventricular septal thickness (4.59 *vs.* 2.15; P<0.05), increased relative interventricular septal thickness (1.00 *vs.* 0.79; P<0.05), and decreased ejection fraction

(81.5% *vs.* 94.6%; P<0.05). These results show that our preparation method is achievable and can successfully establish a rat model of cardiac hypertrophy.

There is no fixed value for the normal range of ejection fraction in rats, and there are significant differences in the literature, which may be caused by differences in rat species, age, and measurement errors (13-15). The HR of the rats did not change significantly during the modeling process, which should be related to the impact of the cardiac function caused by artificially adjusting the dose of anesthetic drugs for each rat when collecting ultrasound data. Our experiments also found that the thickening of the ventricular septum in rats is more evident than that of the posterior wall of the left ventricle, showing asymmetric hypertrophy, which is the same outcome as the study by Rodrigues *et al.* The specific reason for the asymmetric thickening is not apparent, which may be related to the more sympathetic nerve distribution in the ventricular septum than the posterior wall. Some scholars have
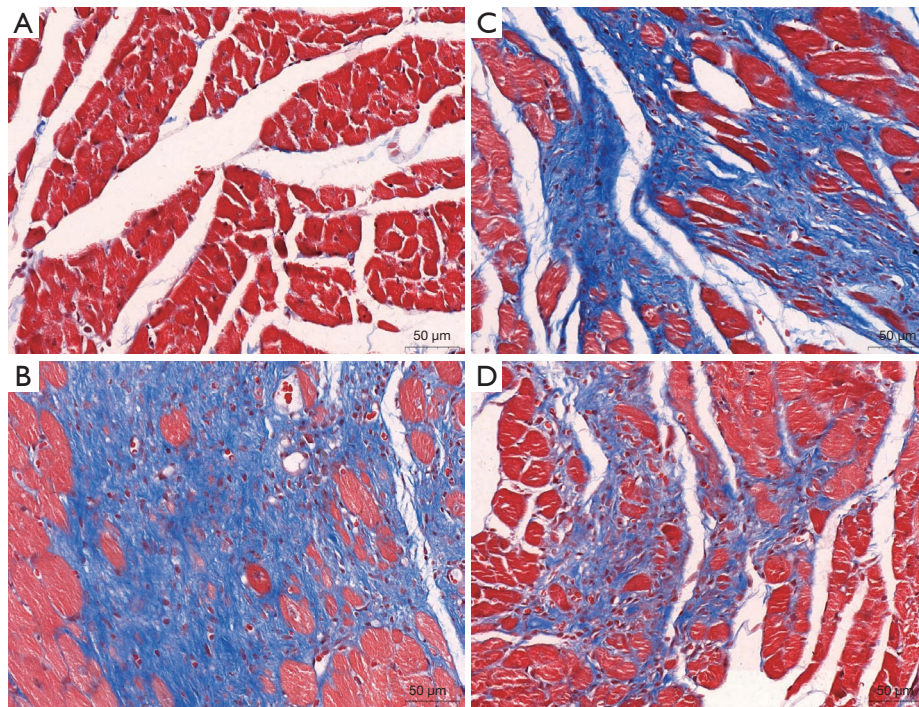
Figure 3 The results of Masson staining of myocardial pathology in four groups of rats. (A) Rats in group A (muscle fibers were arranged neatly); (B) rats in group B (significant deposition of interstitial fibers, disordered and significantly reduced muscle fibers); (C) rats in group C (more obvious deposition of interstitial fibers, the arrangement of muscle fibers is slightly disordered); (D) rats in group D (the interstitial fibers are less deposited, and the muscle fibers are arranged more neatly).

suggested that this may be related to the angiotensin II receptor subtype, which has been shown to mediate protein synthesis in rats and cardiomyocytes hypertrophy (16).

Echocardiography is still a recognized non-invasive examination method that could provide a reliable and accurate evaluation of cardiac function. LVEF is a commonly used index for clinical evaluation of left ventricular systolic function, and it can reflect left ventricular pumping function. It cannot reflect the inherent contractile characteristics of the myocardium, so it has no advantage in identifying early myocardial contractile dysfunction and evaluating the efficacy of short-term drug intervention (17). The left ventricular myocardium of an ordinary person is composed of three layers of myocardium, the endocardial myocardium, the middle myocardium and the epicardial myocardium. The movement of the left ventricular myocardium can be divided into longitudinal, radial, and circular movements (18). The layered strain technology is developed on the basis of the two-dimensional speckle-tracking imaging technology (2D-STI), which automatically tracks the three-layer myocardial acoustic speckles to obtain the strain values of

different myocardial layers, and quantitatively evaluate the influence of the disease on the strain of each layer of the left ventricle to understand the degree of myocardial involvement in detail. In myocardial ischemia, the degree of damage of the inner, middle and outer myocardium of the ventricular wall is different, and this has become the theoretical basis for evaluating the function of myocardial stratification (19). The layered strain technology has the advantage of accurate and rapid assessment of myocardial movement without angle dependence, and has recently become a newly emerging technology to assess myocardial function, especially systolic function under pathological conditions (13).

We found that the CS was more sensitive than LV ejection fraction in assessing early myocardial injury in cardiac hypertrophy in our animal model, which was also confirmed by histopathological examination. In our study, compared with group A, the EF values of groups B, C, and D did not decrease on day 7, while the absolute values of Endo-CS and Mid-CS were lower. This result may have been obtained because at the beginning of ventricular remodeling, in order to continue to maintain the normal
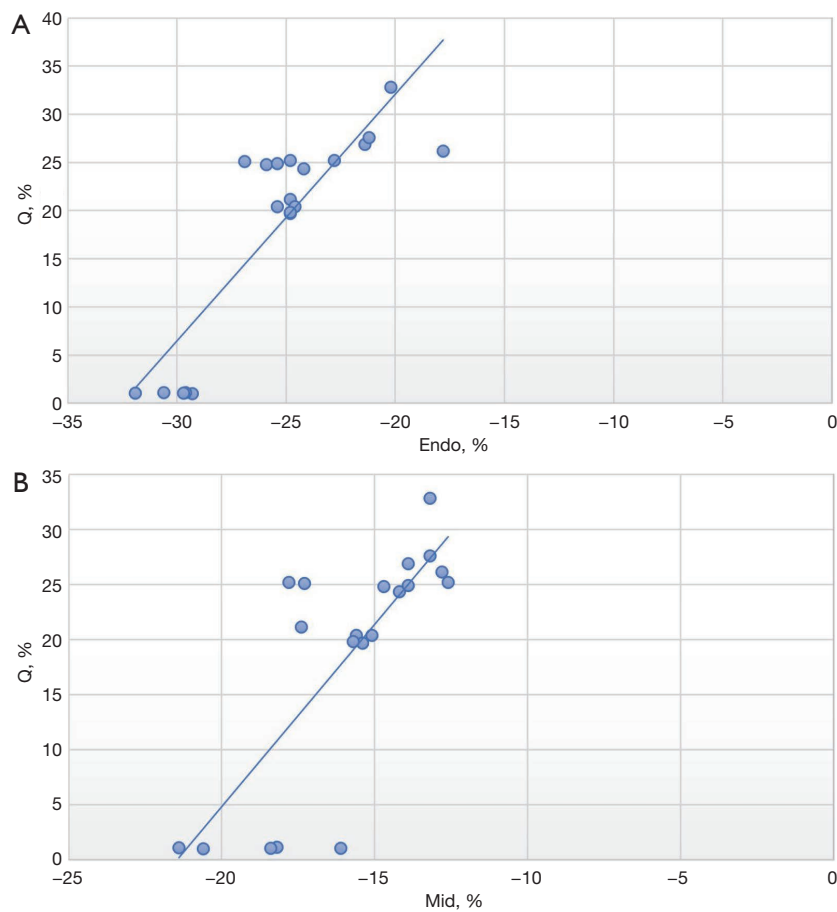
Figure 4 Scatter plots. (A) Scatter plot of Endo-CS and percentage of myocardial interstitial fiber deposition; (B) scatter plot of Mid-CS and percentage of myocardial interstitial fiber deposition. Endo, endocardial myocardium; Mid, midwall myocardium; CS, circumferential strain.

Table 4 Comparison of Rho/ROCK signaling pathway in four groups of rats

Groups	ROCK	RhoA	Bax	Bcl-2
A	0.18±0.02	0.17±0.02	0.18±0.03	0.49±0.03
B	0.47±0.04	0.41±0.03	0.48±0.03	0.15±0.03
C	0.36±0.03	0.35±0.03	0.37±0.03	0.28±0.02
D	0.25±0.04	0.24±0.03	0.26±0.02	0.35±0.02
P value	<0.001	<0.001	<0.001	<0.001

Data are shown as mean ± standard deviation.

ejection function of the left ventricle, the myocardial cells will increase in response, and the ventricular wall will also compensatorily thicken, so as to better maintain the contractility of the left ventricle (20). We also found that the Endo-CS and Mid-CS of the three groups B, C, and D were significantly lower than those of the control group, while the Epi-CS did not significantly decrease. This may be due to the fact that the subendocardial myocardium is most vulnerable to factors such as myocardial ischemia. Firstly, there is an abnormal deposition of the collagen matrix, increased collagen fibers and disordered arrangement, as well as the subepicardial myocardium is relatively less
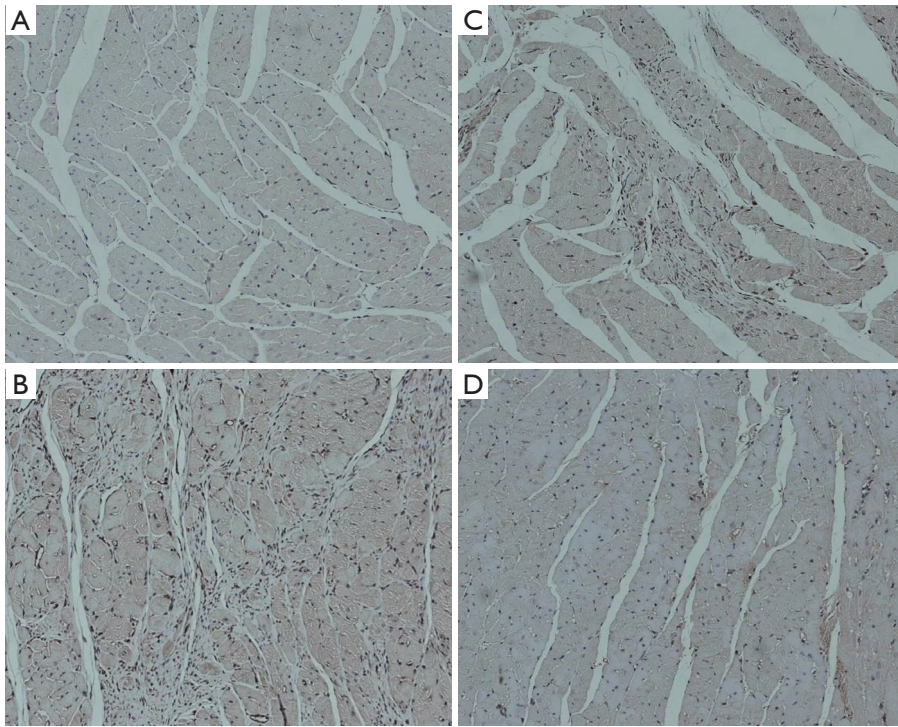
Figure 5 Expression of ROCK protein in four groups of rats. Immunohistochemical staining, ×100. (A) Rats in group A; (B) rats in group B (positive, with a large amount of brown granular ROCK protein); (C) rats in group C; (D) rats in group D.
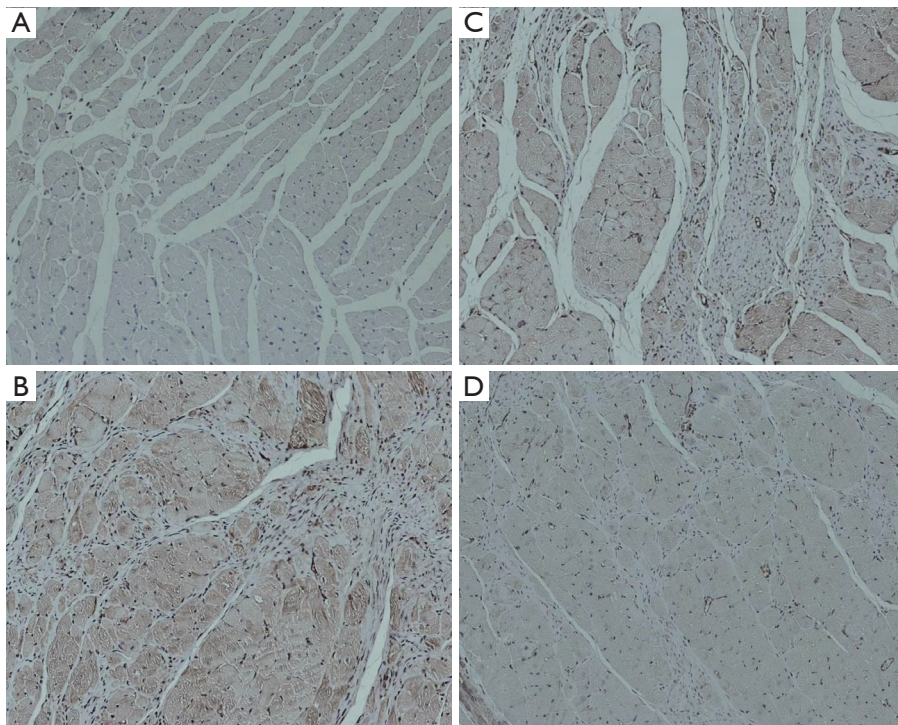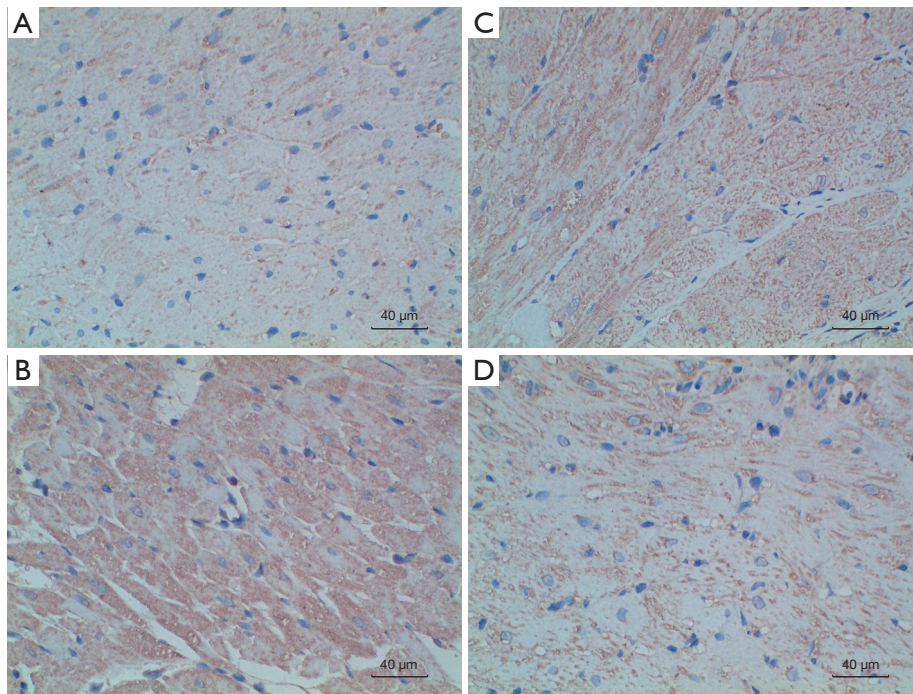

Figure 6 Expression of RhoA protein in four groups of rats. Immunohistochemical staining, ×100. (A) Rats in group A; (B) rats in group B (positive, with a large amount of brown granular RhoA protein); (C) rats in group C; (D) rats in group D.
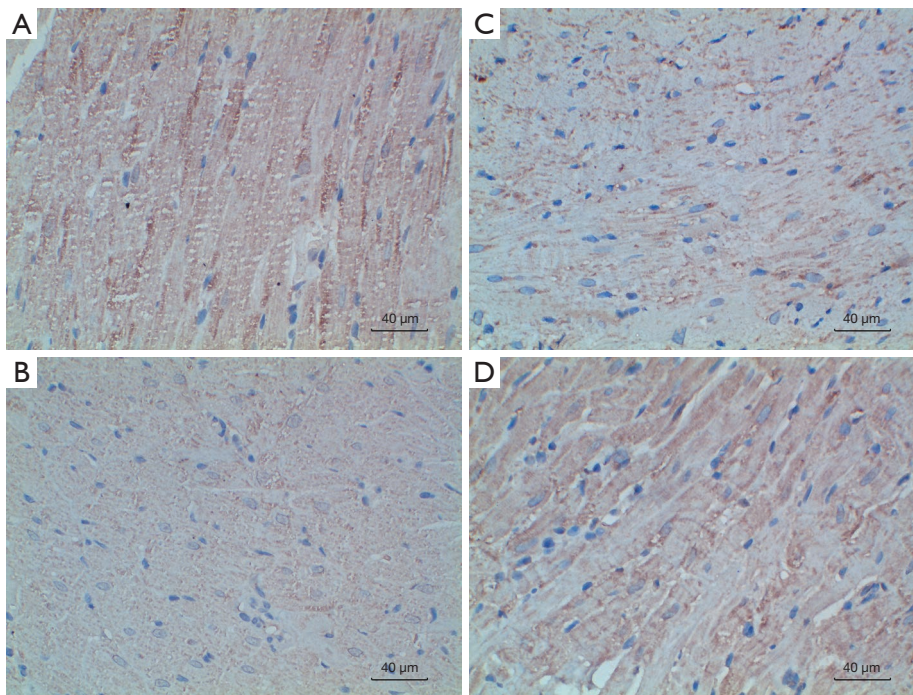
Figure 7 Expression of Bax protein in four groups of rats. Immunohistochemical staining, ×100. (A) rats in group A; (B) rats in group B (positive, with a large amount of brown granular Bax protein); (C) rats in group C; (D) rats in group D.

Figure 8 Expression of Bcl-2 protein in four groups of rats. Immunohistochemical staining, ×100. (A) Rats in group A; (B) rats in group B (positive, with a large amount of brown granular Bcl-2 protein); (C) rats in group C; (D) rats in group D.

affected. Generally, subendocardial contractile forces are higher than subepicardial, but simultaneously, they are more vulnerable to injury due to their relatively high energy requirements (21). Our results confirm that CS may be more likely to induce subtle changes in left ventricular mechanics as cardiac hypertrophy progresses. Previous study has shown that when the heart is under a hemodynamic burden, the heart can use the Frank-Starling mechanism to increase muscle mass and use neurohormonal mechanisms to compensate (22). The layered strain results revealed that the CS in the three groups showed a downward trend from subendocardial to subepicardial, and the differences in the interlayer strain values were statistically significant. This may be because the width of cardiomyocytes increases from the subendocardium to the middle layer, and the myosin phenotype in the subendocardium and the middle layer is also different from that in the subpericardium. Not only is the structure uneven, but the mechanical state of the myocardium is also uneven. The stress of the subendocardial end-diastolic myocardium was increased, and the relative motion amplitude was greater than that of the subepicardial myocardium (23,24). Additionally, our Spearman rank correlation analysis results showed that Endo-CS was positively correlated with the percentage of myocardial interstitial fiber deposition (r=0.805, P<0.001), and Mid-CS was positively correlated with the percentage of myocardial interstitial fiber deposition (r=0.758, P<0.001), indicating that CS, especially Endo-CS and Mid-CS, can correctly assess the severity of myocardial fibrosis that is consistent with the pathological results. Conclusively, the CS of the left ventricular subendocardial layer may be more sensitive to changes in myocardial function and can reflect myocardial dysfunction earlier. Compared with traditional imaging methods, 2D-STI-based layered strain techniques can provide patients with more comprehensive information on subclinical myocardial dysfunction earlier.

Compared with group B, the structure and function indexes of conventional echocardiography in groups C and D did not change significantly, but Endo-CS and Mid-CS increased, which was more significant in group D, and the difference was statistically significant. It has been proved that BBR can effectively improve the systolic function of the left ventricular subendocardial myocardium and middle myocardium in rats with cardiac hypertrophy. This mechanism may be related to the ratio of endocardium to myocardial work, and myocardial oxygen consumption is positively correlated with myocardial work. Additionally, myocardial tissue hematoxylin and eosin (H&E) staining

and Masson staining showed that myocardial tissue inflammation and fibrosis were reduced after BBR intervention, further demonstrating that BBR can slow the progression of fibrosis. Simultaneously, HW/BW decreased (3.70 *vs.* 3.18, 3.70 *vs.* 2.76, P<0.001), suggesting that BBR had a particular protective effect on the myocardium, and the higher dose was more prominent. STI-stratified strain can identify these subtle interlayer changes and could quantitatively evaluate the impact of short-term drug intervention. In this study, on the basis of confirming the protective effect of BBR on cardiac hypertrophy, we further explored the potential mechanism of BBR in slowing down the progression of cardiac hypertrophy.

The RhoA/ROCK pathway is involved in various cardiovascular diseases (25), such as heart failure, and may also be very involved in ISO-induced cardiac hypertrophy (26). Tian *et al.* confirmed that the ROCK inhibitor BBR has cardioprotective effects in a model of myocardial infarction, and is considered a novel adjuvant therapy to reduce myocardial injury (27). Oxidative stress is a harmful process that can be an essential mediator of cellular structural damage, thereby inducing various disease states, such as cardiovascular disease, cancer, neurological disorders, and diabetes (28). ROCK-1 is deemed to be the most central member of the Rho/ROCK signaling pathway. Due to the relationship between ROCK-1 and cardiomyocyte remodeling, we conducted this study to evaluate the effect of the ROCK inhibitor BBR on cardiac hypertrophy in rats, and to dig deeper into its specific mechanism of action at the protein level for future early treatment to develop effective strategies and provide research direction. The results of this study showed that compared with group A, the expression of ROCK and RhoA proteins in groups B, C, and D were enhanced. The above results proved that ISO significantly increased the expressions of ROCK-1 protein and RhoA protein in rat cardiomyocytes, indicating that Rho/ROCK is involved in ISO-induced cardiac hypertrophy, while the early intervention of BBR reduced ROCK-1 protein and RhoA protein The expression of BBR hydrochloride can oppose the Rho/ROCK signaling pathway to improve ISO-induced cardiac hypertrophy.

Our experimental results showed that compared with group A, the expression of Bax protein in groups B, C, and D was enhanced, while the expression of Bcl-2 protein was significantly reduced. increase, prove that ISO inhibits the expression of Bcl-2, BBR increases the expression of Bcl-2, prove that BBR inhibits oxidative stress by increasing the expression of anti-apoptotic genes, and BBR pre-treatment

can slow down ISO. The resulting imbalance of Bax and Bcl-2 protein expression. This result further verifies that the Rho/ROCK signaling pathway is involved in ISO-induced cardiac hypertrophy in rats. BBR hydrochloride can counteract the Rho/ROCK signaling pathway, and the downstream target factors such as Bax and Bcl-2 change and inhibit oxidation. Simultaneously, in our study, the expression of Bcl-2 protein in group D was higher than that in group C, which proved that the early intervention effect of high-dose BBR was more prominent.

Altogether, this study demonstrates that ISO may induce cardiac hypertrophy through the Rho/ROCK signaling pathway, which in turn leads to cardiomyocyte apoptosis. However, BBR hydrochloride inhibited oxidative stress by increasing the expression of the anti-apoptotic gene Bcl-2, and effectively inhibited the excessive activation of ROCK-1, achieving the effect of early intervention to improve cardiac hypertrophy, which provides a direction for further exploration of the specific mechanism in the future.

Critique of study

This study had several limitations. (I) The doses of BBR used in this experiment were 5 and 10 mg/kg/day, and the duration of the medication was relatively short. Therefore, it was necessary to increase the observation of drug course, and at the same time to investigate whether the reduction of EF value occurred in the rats with reduced layered strain value; this should be explored in future experiments. (II) The rat was small and cannot accurately divide the three parts of the short axis of the left ventricle. To ensure the maximum possible accuracy of the measurement, only the most obvious left ventricle was selected Image of papillary muscle level. (III) The number of experimental cases was small, and the correlation between stratified strain and clinical application of BBR need to be further confirmed in large-scale clinical trials in the future. (IV) The expression of Rho/ROCK signaling pathway-related proteins was only detected by immunohistochemistry, and the molecular level was not involved. In future experiments, fluorescence quantitative PCR and Western Blot methods will be added for further exploration.

Conclusions

To our knowledge, this was the first study to use layered strain to assess systolic function before and after BBR intervention in a rat model of cardiac hypertrophy.

According to our research results, STI-layered strain technology can evaluate the changes of left ventricular systolic function in the early stage of ISO-induced cardiac hypertrophy in rats, and for cardiac hypertrophy rats, the subendocardial myocardial injury is the most serious, and STI layered strain imaging technology is in the detection of cardiac hypertrophy. It is more sensitive to early cardiac injury mediated by cardiac hypertrophy; BBR can act on the Rho/ROCK signaling pathway, exert its inhibitory effect, reduce the expression of ROCK protein in the myocardial tissue of rats with cardiac hypertrophy, and regulate its downstream target factor Bax, Bcl-2 expression, inhibiting oxidative stress, thereby improving myocardial hypertrophy, STI layered strain imaging technology could evaluate the efficacy of short-term drug intervention. The specific mechanism needs to be further studied and discovery.

Footnote

Reporting Checklist: The authors have completed the ARRIVE reporting checklist. Available at https://cdt.amegroups.com/article/view/10.21037/cdt-22-464/rc

Data Sharing Statement: Available at https://cdt.amegroups.com/article/view/10.21037/cdt-22-464/dss

Peer Review File: Available at https://cdt.amegroups.com/article/view/10.21037/cdt-22-464/prf

Conflicts of Interest: All authors have completed the ICMJE uniform disclosure form (available at https://cdt.amegroups.com/article/view/10.21037/cdt-22-464/coif). The authors have no conflicts of interest to declare.

Ethical Statement: The authors are accountable for all

aspects of the work in ensuring that questions related to the accuracy or integrity of any part of the work are appropriately investigated and resolved. Experiments were performed under a project license (No. 27-2021) granted by the Ethics Committee of University of Electronic Science and Technology of China, in compliance with our institutional guidelines for the care and use of animals.

Open Access Statement: This is an Open Access article distributed in accordance with the Creative Commons Attribution-NonCommercial-NoDerivs 4.0 International License (CC BY-NC-ND 4.0), which permits the non-commercial replication and distribution of the article with the strict proviso that no changes or edits are made and the original work is properly cited (including links to both the formal publication through the relevant DOI and the license). See: https://creativecommons.org/licenses/by-nc-nd/4.0/.

References

1. Iismaa SE, Li M, Kesteven S, et al. Cardiac hypertrophy limits infarct expansion after myocardial infarction in mice. Sci Rep 2018;8:6114.
2. Nakamura M, Sadoshima J. Mechanisms of physiological and pathological cardiac hypertrophy. Nat Rev Cardiol 2018;15:387-407.
3. Bai XJ, Hao JT, Wang J, et al. Curcumin inhibits cardiac hypertrophy and improves cardiovascular function via enhanced Na(+)/Ca(2+) exchanger expression after transverse abdominal aortic constriction in rats. Pharmacol Rep 2018;70:60-8.
4. Pastore MC, De Carli G, Mandoli GE, et al. The prognostic role of speckle tracking echocardiography in clinical practice: evidence and reference values from the literature. Heart Fail Rev 2021;26:1371-81.
5. Tokodi M, Oláh A, Fábián A, et al. Novel insights into the athlete's heart: is myocardial work the new champion of systolic function? Eur Heart J Cardiovasc Imaging 2022;23:188-97.
6. Tsugu T, Postolache A, Dulgheru R, et al. Echocardiographic reference ranges for normal left ventricular layer-specific strain: results from the EACVI NORRE study. Eur Heart J Cardiovasc Imaging 2020;21:896-905.
7. Morariu VI, Arnautu DA, Morariu SI, et al. 2D speckle tracking: a diagnostic and prognostic tool of paramount importance. Eur Rev Med Pharmacol Sci 2022;26:3903-10.
8. Aksu U, Uzun MH. A new era: Speckle tracking echocardiography and cardiomyopathies. J Clin Ultrasound 2022;50:1249-50.
9. Moreau S, DaSilva JN, Valdivia A, et al. N-[(11)C]-methyl-hydroxyfasudil is a potential biomarker of cardiac hypertrophy. Nucl Med Biol 2015;42:192-7.
10. Wu X, Liu Z, Yu XY, et al. Autophagy and cardiac diseases: Therapeutic potential of natural products. Med Res Rev 2021;41:314-41.
11. Che Y, Shen DF, Wang ZP, et al. Protective role of berberine in isoprenaline-induced cardiac fibrosis in rats. BMC Cardiovasc Disord 2019;19:219.
12. Tian L, Ri H, Qi J, et al. Berberine elevates mitochondrial membrane potential and decreases reactive oxygen species by inhibiting the Rho/ROCK pathway in rats with diabetic encephalopathy. Mol Pain 2021;17:1744806921996101.
13. Hua Y, Xie M, Yin J, et al. Evaluation of effect of atorvastatin on left ventricular systolic function in rats with myocardial infarction via 2D-STI technique. Exp Ther Med 2018;15:4386-94.
14. Li MH, Zhang YJ, Yu YH, et al. Berberine improves pressure overload-induced cardiac hypertrophy and dysfunction through enhanced autophagy. Eur J Pharmacol 2014;728:67-76.
15. Zhang H, Sun Y, Liu X, et al. Speckle tracking echocardiography in early detection of myocardial injury in a rat model with stress cardiomyopathy. Med Ultrason 2019;21:441-8.
16. Rodrigues JC, Amadu AM, Dastidar AG, et al. Prevalence and predictors of asymmetric hypertensive heart disease: insights from cardiac and aortic function with cardiovascular magnetic resonance. Eur Heart J Cardiovasc Imaging 2016;17:1405-13.
17. Scharrenbroich J, Hamada S, Keszei A, et al. Use of two-dimensional speckle tracking echocardiography to predict cardiac events: Comparison of patients with acute myocardial infarction and chronic coronary artery disease. Clin Cardiol 2018;41:111-8.
18. Ma C, Fan J, Zhou B, et al. Myocardial strain measured via two-dimensional speckle-tracking echocardiography in a family diagnosed with arrhythmogenic left ventricular cardiomyopathy. Cardiovasc Ultrasound 2021;19:40.
19. Aurich M, Keller M, Greiner S, et al. Left ventricular mechanics assessed by two-dimensional echocardiography and cardiac magnetic resonance imaging: comparison of high-resolution speckle tracking and feature tracking. Eur Heart J Cardiovasc Imaging 2016;17:1370-8.
20. Boraita A, Díaz-Gonzalez L, Valenzuela PL, et al. Normative Values for Sport-Specific Left Ventricular

Dimensions and Exercise-Induced Cardiac Remodeling in Elite Spanish Male and Female Athletes. Sports Med Open 2022;8:116.

21. Ishizu T, Seo Y, Kameda Y, et al. Left ventricular strain and transmural distribution of structural remodeling in hypertensive heart disease. Hypertension 2014;63:500-6.

22. Xu L, Wang N, Chen X, et al. Quantitative evaluation of myocardial layer-specific strain using two-dimensional speckle tracking echocardiography among young adults with essential hypertension in China. Medicine (Baltimore) 2018;97:e12448.

23. Toepfer CN, Garfinkel AC, Venturini G, et al. Myosin Sequestration Regulates Sarcomere Function, Cardiomyocyte Energetics, and Metabolism, Informing the Pathogenesis of Hypertrophic Cardiomyopathy. Circulation 2020;141:828-42.

24. Chen J, Liu W, Zhang H, et al. Regional ventricular wall thickening reflects changes in cardiac fiber and sheet structure during contraction: quantification with diffusion tensor MRI. Am J Physiol Heart Circ Physiol 2005;289:H1898-907.

25. Dokumacioglu E, Duzcan I, Iskender H, et al. RhoA/ROCK-1 Signaling Pathway and Oxidative Stress in Coronary Artery Disease Patients. Braz J Cardiovasc Surg 2022;37:212-8.

26. Wang P, Xu S, Xu J, et al. Elevated MCU Expression by CaMKIIδB Limits Pathological Cardiac Remodeling. Circulation 2022;145:1067-83.

27. Tian CX, Li MY, Shuai XX, et al. Berberine plays a cardioprotective role by inhibiting macrophage Wnt5a/β-catenin pathway in the myocardium of mice after myocardial infarction. Phytother Res 2023;37:50-61.

28. Soares DDS, Pinto GH, Lopes A, et al. Cardiac hypertrophy in mice submitted to a swimming protocol: influence of training volume and intensity on myocardial renin-angiotensin system. Am J Physiol Regul Integr Comp Physiol 2019;316:R776-82.